Vol. 52: 7–29, 2012
doi: 10.3354/cr01018

CLIMATE RESEARCH
Clim Res

Published March 22

Contribution to CR Special 29 'The regional climate model RegCM4'

RegCM4: model description and preliminary tests over multiple CORDEX domains

F. Giorgi[1,*], E. Coppola[1], F. Solmon[1], L. Mariotti[1], M. B. Sylla[1], X. Bi[1], N. Elguindi[1], G. T. Diro[1], V. Nair[1], G. Giuliani[1], U. U. Turuncoglu[1], S. Cozzini[2], I. Güttler[3], T. A. O'Brien[4], A. B. Tawfik[5], A. Shalaby[6], A. S. Zakey[7], A. L. Steiner[5], F. Stordal[8], L. C. Sloan[4], C. Brankovic[3]

[1]Earth System Physics Section, International Centre for Theoretical Physics, 34151 Trieste, Italy
[2]Consiglio Nazionale delle Ricerche, 34100 Trieste, Italy
[3]Croatian Meteorological Service, Zagreb, Croatia
[4]University of California, Santa Cruz, California 95064, USA
[5]University of Michigan, Ann Arbor, Michigan 48109, USA
[6]Cairo University, Cairo, Egypt
[7]Danish Meteorological Institute, Copenhagen, Denmark
[8]University of Oslo, Oslo, Norway

ABSTRACT: A new version of the RegCM regional climate modeling system, RegCM4, has been recently developed and made available for public use. Compared to previous versions, RegCM4 includes new land surface, planetary boundary layer, and air–sea flux schemes, a mixed convection and tropical band configuration, modifications to the pre-existing radiative transfer and boundary layer schemes, and a full upgrade of the model code towards improved flexibility, portability, and user friendliness. The model can be interactively coupled to a 1D lake model, a simplified aerosol scheme (including organic carbon, black carbon, SO_4, dust, and sea spray), and a gas phase chemistry module (CBM-Z). After a general description of the model, a series of test experiments are presented over 4 domains prescribed under the CORDEX framework (Africa, South America, East Asia, and Europe) to provide illustrative examples of the model behavior and sensitivities under different climatic regimes. These experiments indicate that, overall, RegCM4 shows an improved performance in several respects compared to previous versions, although further testing by the user community is needed to fully explore its sensitivities and range of applications.

KEY WORDS: RegCM4 · Regional climate model · CORDEX · Model validation

1. INTRODUCTION

Interest in regional climate modeling has been steadily increasing in the last 2 decades (e.g Giorgi 2006). As a result, a number of regional climate models (RCMs) have been developed, with a wide base of model users. One such RCM is the RegCM system, which has evolved from the first version developed in the late 1980s (RegCM1; Dickinson et al. 1989, Giorgi 1990) to later versions in the early 1990s (RegCM2; Giorgi et al. 1993a,b), late 1990s (RegCM2.5; Giorgi & Mearns 1999), and 2000s (RegCM3; Pal et al. 2007). The RegCM was the first limited area model developed for long-term regional climate simulation: it has been used in numerous regional model intercomparison projects, and it has been applied by a large community for a wide range of regional climate studies, from process studies (Qian 2008, Qian et al. 2010) to paleo-climate and future climate projections (Giorgi & Mearns 1999, Giorgi et al. 2006).

The RegCM system is a community model, and in particular it is designed for use by a varied commu-

*Email: giorgi@ictp.it

nity composed of scientists in industrialized countries as well as developing nations (Pal et al. 2007). As such, it is designed to be a public, open source, user-friendly, and portable code that can be applied to any region of the world. It is supported through the Regional Climate Research Network, or RegCNET, a widespread network of scientists coordinated by the Earth System Physics section of the Abdus Salam International Centre for Theoretical Physics (ICTP; Giorgi et al. 2006; http://users.ictp.it/RegCNET/). Scientists across this network (currently >750 participants) can communicate through an email list and via regular scientific workshops, and they have been essential for the evaluation and sequential improvements of the model.

Since the release of RegCM3, described by Pal et al. (2007), the model has undergone a substantial evolution both in terms of software code and physics representations, and this has led to the development of a fourth version of the model, RegCM4, which was released by the ICTP in June 2010 as a prototype version (RegCM4.0) and in April 2011 as a first complete version (RegCM4.1). The purpose of the present study is to provide a basic reference for RegCM4 including both the description of the model improvements and a limited illustrative analysis of the model behavior and sensitivities in different climatic regimes. Other articles in this Theme Section (TS) will present more extensive and detailed studies with RegCM4, along with applications using the earlier version of the model.

In Section 2 we first describe the main model developments along with a summary of all the different available model options. Section 3 then presents a basic analysis of a set of experiments aimed at illustrating the model performance and sensitivities. These experiments were carried out over a sub-set of the standard domains recommended by the newly developed international coordinated regional climate downscaling experiment (CORDEX) project (Giorgi et al. 2009; http://wcrp.ipsl.jussieu.fr/SF_RCD_CORDEX.html) using reanalyses of observations to drive the model at the lateral boundaries for multi-annual simulation periods. Only a basic set of simple performance metrics was used for the evaluation of the model, with more comprehensive metrics and analysis being left to other contributions to this special issue. Finally, Section 4 provides a discussion of the status of the model and future plans for its development and application.

2. DESCRIPTION OF RegCM4

RegCM4 is an evolution of its previous version, RegCM3, described by Pal et al. (2007). In this section, we summarize the basic features of RegCM4, highlighting the main changes with respect to RegCM3. Table 1 presents a list of the options available in the model and can be used as reference for the following sections.

2.1. Model dynamics

The basic model dynamics have remained the same as in RegCM3, which was essentially the same as that of the previous version RegCM2 (Giorgi et al. 1993a,b). RegCM4 is thus a hydrostatic, compressible, sigma-p vertical coordinate model run on an Arakawa B-grid in which wind and thermodynamical

Table 1. Model options available in RegCM4. PBL: planetary boundary layer

Model aspects	Available options
Dynamics	• Hydrostatic, σ-vertical coordinate (Giorgi et al. 1993a)
Radiative transfer	• Modified CCM3 (Kiehl et al. 1996)
PBL	• Modified Holtslag (Holtslag et al. 1990) • UW-PBL (Bretherton et al. 2004)
Cumulus convection	• Simplified Kuo (Anthes et al. 1987) • Grell (Grell 1993) • MIT (Emanuel & Zivkovic-Rothman 1999) • Tiedtke (Tiedtke 1989)
Resolved scale precipitation	• SUBEX (Pal et al. 2000)
Land surface	• BATS (Dickinson et al. 1993) • Sub-grid BATS (Giorgi et al. 2003) • CLM (Steiner et al. 2009)
Ocean fluxes	• BATS (Dickinson et al. 1993) • Zeng (Zeng et al. 1998) • Diurnal sea surface temperature (Zeng & Beljaars 2005)
Interactive aerosols	• Organic and black carbon, SO_4 (Solmon et al. 2006) • Dust (Zakey et al. 2006) • Sea salt (Zakey et al. 2008)
Interactive lake	• 1D diffusion/convection (Hostetler et al. 1993)
Tropical band	• Coppola et al. (2012, this Special)
Coupled ocean (not in public version)	• MIT (Artale et al. 2010) • ROMS (Ratnam et al. 2009)

variables are horizontally staggered. A time-splitting explicit integration scheme is used in which the 2 fastest gravity modes are first separated from the model solution and then integrated with smaller time steps. This allows the use of a longer time step for the rest of the model. Essentially, the model dynamics are the same as that of the hydrostatic version of MM5 (Grell et al. 1994), and since this has not changed in RegCM4, it is not further discussed here (see Giorgi et al. 1993a and Grell et al. 1994 for more details).

2.2. Model physics

2.2.1. Radiative transfer

Radiative transfer calculations in RegCM4 are carried out with the radiative transfer scheme of the global model CCM3 (Kiehl et al. 1996), as implemented by Giorgi et al. (1999). This includes calculations for the short-wave and infrared parts of the spectrum, including both atmospheric gases and aerosols. The scheme includes contributions from all main greenhouse gases, i.e. H_2O, CO_2, O_3, CH_4, N_2O, and CFCs, and solar radiative processes are treated using a delta-Eddington formulation (Briegleb 1992). Scattering and absorption of solar radiation by aerosols are also included based on the aerosol optical properties (absorption coefficient and single scattering albedo).

Concerning cloud radiation calculations, the solar spectrum optical properties are based on the cloud liquid water path, which is in turn based on the cloud liquid water amount prognostically calculated by the model (see Section 2.2.4), cloud fractional cover, which is calculated diagnostically as a function of relative humidity, and effective cloud droplet radius, which is parameterized as a function of temperature and land sea mask for liquid water and as a function of height for ice phase. In addition, the scheme diagnostically calculates a fraction of cloud ice as a function of temperature. In the infrared spectrum, the cloud emissivity is calculated as a function of cloud liquid/ice water path and cloud infrared absorption cross sections depending on effective radii for the liquid and ice phases.

One of the problems in this formulation is that the scheme uses the cloud fractional cover to produce grid box mean cloud properties which are then treated as though the entire grid box were covered by an effectively thinner cloud layer. However, because of the non-linear nature of radiative transfer, this approach tends to produce a 'grayer' mean grid box than if separate cloudy and clear sky fractional fluxes were calculated. By taking advantage of the fact that the scheme also calculates clear sky fluxes for diagnostic purposes, in RegCM4 we modified this radiative cloud representation by first calculating the total cloud cover at a given grid point and then calculating the surface fluxes separately for the cloudy and clear sky portions of the grid box. The total cloud cover at a model grid box is given by a value intermediate between that obtained using the random overlap assumption (which maximizes cloud cover) and that given by the largest cloud cover found in any single layer of the column overlying the grid box (which implies a full overlap and it is thus is a minimum estimate of total cloud cover). This modification thus accounts for the occurrence of fractional clear sky at a given grid box, leading to more realistic grid-box average surface radiative fluxes in fractional cloudy conditions.

The other main development compared to RegCM3 concerns the aerosol radiative transfer calculations. In RegCM3, the aerosol radiative forcing was based on 3-dimensional fields produced by the aerosol model (see below), and included only scattering and absorption in the shortwave spectrum (see Giorgi et al. 2002). In RegCM4, we added the contribution of the infrared spectrum following Solmon et al. (2008). This is especially important for relatively large dust and sea salt particles, and it is calculated by introducing an aerosol infrared emissivity calculated as a function of the aerosol path and absorption cross section estimated from aerosol size distribution and long-wave refractive indices. Long-wave diffusion, which could be relevant for larger dust particles, is not treated as part of this scheme.

2.2.2. Planetary boundary layer

Two major developments have occurred in RegCM4 concerning the description of planetary boundary layer (PBL) processes. First, the scheme currently available in the RegCM system, that of Holtslag et al. (1990), underwent various modifications, and second a new PBL scheme, the University of Washington PBL (Grenier & Bretherton 2001, Bretherton et al. 2004), was implemented in the model.

In the Holtslag scheme, a PBL height is first diagnostically calculated based on an iteration procedure employing a bulk critical Richardson number formulation. Then a non-local vertical profile of eddy diffusivity for heat, moisture, and momentum is specified from the surface to the PBL height, and a countergradient transport term is added for temperature and moisture. The eddy diffusivity depends on the friction velocity, height, Monin-Obhukov length, and PBL height.

Compared to other schemes, this formulation tends to produce relatively strong, and often excessive, turbulent vertical transfer. For example, after extensive testing, we found excessive vertical transfer of moisture in the model resulting in low moisture amounts near the surface and excessive moisture near the PBL top. Therefore in order to ameliorate this problem, the countergradient term for water vapor was removed in RegCM4. Another problem of the Holtslag scheme (at least in our implementation) is an excessive vertical transport of heat, moisture, and momentum in very stable conditions, such as during the winter in northern hemisphere high latitude regions. For example, we found that in such conditions, the scheme fails to simulate near-surface temperature inversions. This in turn leads to large warm winter biases (>10°C) over regions such as northern Siberia and northern Canada. As an ad hoc fix to address this problem, in RegCM4 we implemented the following modification to the scheme. We first defined 'very stable' conditions within the Holtslag parameterization as conditions in which the ratio of the height from the surface over the Monin-Obhukov length is lower than 0.1. When such conditions were found, we set the eddy diffusivity and counter-gradient terms for all variables to 0. Preliminary tests showed that this modification reduces the warm bias in high latitude winter conditions and allows the model to better capture surface inversions. These modifications have thus been incorporated as default in the RegCM4 code.

One of the deficiencies identified in RegCM3 has been the lack of simulation of low level stratus clouds, a problem clearly tied to the excessive vertical transport in the Holtslag PBL scheme (T. A. O'Brien et al. unpubl.). To address this problem, T. A. O'Brien et al. (unpubl.) coupled the general turbulence closure parameterization of Grenier & Bretherton (2001) and Bretherton et al. (2004) to the RegCM4, which we refer to as UW-PBL. This is a 1.5 order local, down-gradient diffusion parameterization in which the velocity scale is based on turbulent kinetic energy (TKE). The TKE is in turn calculated prognostically from the balance of buoyant production/destruction, shear production, dissipation vertical transport, and horizontal diffusion and advection. The scheme also parameterizes the entrainment process and its enhancement by evaporation of cloudy air into entrained air. The UW-PBL has been so far tested within the RegCM4 framework mostly in mid-latitude domains, such as the continental US (where it considerably improved the simulation of low level stratus clouds; T. A. O'Brien et al. unpubl.) and Europe, and an example of its performance is reported in Section 3.

2.2.3. Cumulus convection

At present, RegCM4 includes 3 options for representing cumulus convection. The first is a simplified version of the Kuo-type scheme of Anthes (1977), as described by Anthes et al. (1987). This scheme has been present since the earliest version RegCM1 and activates convection when the column moisture convergence exceeds a threshold value. This scheme, although still available, is used only very occasionally and generally provides poorer precipitation simulations than the other available parameterizations.

The second, and to date most used scheme, is that of Grell (1993) in the implementation of Giorgi et al. (1993b). This is a mass flux deep convection parameterization in which clouds are considered as 2 steady-state circulations including an updraft and a penetrative downdraft. The scheme is triggered when a parcel lifted in the updraft eventually reaches the moist convection level. A single cloud model is used with entrainment and detrainment only at the cloud bottom and top. Two different closures can be adopted: an Arakawa-Schubert type closure in which all buoyant energy is immediately released at each time step and a Fritsch-Chappell type closure in which the available buoyant energy is released with a time scale typically on the order of 30 min. A number of parameters present in the scheme can be used to optimize its performance, and Giorgi et al. (1993b) discussed a wide range of sensitivity experiments. We found that the parameter to which the scheme is most sensitive is by and large the fraction of precipitation evaporated in the downdraft (Peff, with values from 0 to 1), which essentially measures the precipitation efficiency. Larger values of Peff lead to reduced precipitation. The Grell scheme has been available in the RegCM system since its second version, RegCM2 (Giorgi et al. 1993b), and it is currently the one most used.

A third scheme was introduced in RegCM3 (Pal et al. 2007), the so called MIT scheme (Emanuel 1991, Emanuel & Zivkovic Rothman 1999). In this parameterization, convection is triggered when the level of buoyancy is higher than the cloud base level. Cloud mixing is considered to be episodic and inhomogenous, and convective fluxes are based on a model of sub-cloud-scale updrafts and downdrafts. Precipitation is based on autoconversion of cloud water into rain water and accounts for simplified ice processes. The MIT scheme is the most complex of the 3 and also includes a number of parameters that can be used to optimize the model performance in different climate regimes. Differently from the Grell scheme, however, test experiments did not identify a single parameter to which the model is most sensitive.

A major augmentation in RegCM4 compared to previous versions of the model is the capability of running different convection schemes over land and ocean, a configuration which we refer to as 'mixed convection.' Extensive test experiments showed that different schemes have different performance over different regions, and in particular over land versus ocean areas. For example, the MIT scheme tends to produce excessive precipitation over land areas, especially through the occurrence of very intense individual precipitation events. In other words, once the scheme is activated, it becomes difficult to 'decelerate.' Conversely, we found that the Grell scheme tends to produce excessively weak precipitation over tropical oceans. These preliminary tests suggested that a mixed convection approach by which, for example, the MIT scheme is used over oceans and the Grell scheme over land, might be the most suitable option to pursue, and therefore this option was added to the model. We also note that, as in the previous version (RegCM3) and many other schemes, these cumulus parameterizations tend to maximize rain in the early afternoon, essentially in response to the surface heating by the solar cycle. This often leads to an earlier than observed diurnal precipitation maximum over tropical regions (Diro et al. 2012, this Special).

2.2.4. Resolved scale precipitation

The resolved scale precipitation scheme was not significantly changed in RegCM4 compared to RegCM3, other than in some of the parameter settings. The scheme is essentially based on the SUBEX parameterization of Pal et al. (2000) and includes a prognostic equation for cloud water. It first calculates fractional cloud cover at a given grid point based on the local relative humidity. Then, in the cloudy fraction it uses a Kessler-type bulk formulation in which cloud water is turned into precipitation via an autoconversion and an accretion term. Below-cloud evaporation of falling raindrops is also accounted for based on the local relative humidity and an evaporation rate coefficient. Key sensitivity parameters in this scheme are the in-cloud liquid water threshold for the activation of the autoconversion term (Qth) and the rate of sub-cloud evaporation (Cevap). Greater values of Qth and Cevap lead to decreased precipitation amounts. Traditionally, RegCM3 has shown a tendency to produce excessive precipitation, especially at high resolutions (Im et al. 2010, Torma et al. 2011), and optimizations of these parameters have proven effective in ameliorating this problem (see Torma et al. 2011).

2.2.5. Land surface processes

Since the earliest versions of the RegCM, land surface processes have been described via the Biosphere-Atmosphere Transfer Scheme (BATS) of Dickinson et al. (1993). This scheme, which has been used for many years, includes a 1-layer vegetation module, a 1-layer snow module, a force-restore model for soil temperatures, a 3-layer soil scheme, and a simple surface runoff parameterization. The scheme includes 20 surface types and 12 soil color and soil texture types. In addition, a sub-grid land surface configuration can be used by which each model grid point is divided into a regular sub-grid, and land surface processes are calculated at each sub-grid point taking into account the local land-use and topography (Giorgi et al. 2003). This latter scheme was shown to be especially useful in improving the simulation of the surface hydrologic cycle in mountainous areas (Giorgi et al. 2003).

As a first augmentation, in RegCM4, 2 new land use types were added to BATS to represent urban and suburban environments. Urban development not only modifies the surface albedo and alters the surface energy balance, but also creates impervious surfaces with large effects on runoff and evapotranspiration. These effects can be described by modifying relevant properties of the land surface types in the BATS package, such as maximum vegetation cover, roughness length, albedo, and soil characteristics. For this purpose, we implemented the parameters proposed in Table 1 of Kueppers et al. (2008).

The second major addition to RegCM4 is the option to use the Community Land Model, version CLM3.5 (Tawfik & Steiner 2011). Compared to BATS, CLM is a more advanced package, which is described in detail by Oleson et al. (2004, 2008). It uses a series of biogeophysically-based parameterizations to describe the land–atmosphere exchanges of energy, momentum, water, and carbon. Within each RegCM4 grid cell, CLM3 divides the cell area into a first sub-grid hierarchy composed of land units (glacier, wetland, lake, urban, and vegetated land cover), and a second and third sub-grid hierarchy for vegetated land units, including different snow/soil columns for the different vegetation fractions, and plant functional types (PFTs; Oleson et al. 2004). Biogeophysical processes are calculated for each land unit, column, and PFT separately, and then averaged for return to the atmospheric model. CLM3 biogeophysical calculations include a coupled photosynthesis–stomatal conductance model, in-canopy radiation schemes, revised multi-layer snow parameterizations, and surface hydrology including a distributed river runoff scheme (Oleson et al. 2008). Soil temperature and water content are calculated with the use of a multiple layer model. Being much more complex than BATS, the use of CLM adds about 20% to the computing time necessary to run the model, depending on the fraction of land points in the domain. CLM also has an option for describing interactive vegetation; however, this has not been tested yet within the RegCM4 framework. CLM was shown to substantially affect the land–atmosphere exchanges of moisture and energy and the associated surface climate feedbacks compared to BATS (Steiner et al. 2009).

2.2.6. Ocean–air exchanges

RegCM3 included 2 options to describe ocean–air turbulent exchanges of heat, momentum, and moisture. The first, and oldest available, is the use of the drag-coefficient parameterization included in the BATS package (Dickinson et al. 1993). In RegCM3, Pal et al. (2007) implemented the scheme of Zeng et al. (1998), which is based on a Monin-Obhukov turbulence representation. This scheme was added in order to improve the excessive evaporation over warm tropical oceans found in the BATS option.

By default in RegCM, sea surface temperatures (SST) are prescribed every 6 h from temporally interpolated weekly or monthly SST products. These products, which are produced from satellite retrievals and *in situ* measurements, are representative of the mean temperature in the top few meters of the ocean. However, the actual SST can differ significantly from this mean temperature due to the cool-skin and warm-layer effects described by Fairall et al. (1996). To improve the calculation of diurnal fluxes over the ocean, the prognostic SST scheme described by Zeng & Beljaars (2005) was implemented in RegCM4. The scheme is based on a 2-layer, 1-dimensional heat transfer model, with the top layer representing the upper few millimeters of the ocean which is cooled by net longwave radiation loss and surface fluxes. The bottom layer is 3 m thick, is warmed by solar radiation, and exchanges heat with the top layer. This diurnal SST scheme appears to provide significant, although not major, effects on the model climatology mostly over tropical oceans, for example the Indian Ocean, and it is now used as the default in RegCM4.

2.3. Coupling with other components of the climate system

2.3.1. Lakes and oceans

In terms of climate system component coupling, the RegCM system includes an interactive 1-dimensional thermal lake model which has been applied in different regional settings (e.g. Hostetler et al. 1993, Small et al. 1999). Different versions of RegCM3 have also been coupled with regional ocean models for specific applications. Artale et al. (2010) coupled RegCM3 with the MIT ocean model (Marshall et al. 1997a,b) towards the development of a regional Earth System model for the Mediterranean basin (the PROTHEUS system). In a separate effort, Ratnam et al. (2009) coupled RegCM3 with the ROMS regional ocean model (Shchepetkin & McWilliams 2005) over a portion of the Indian Ocean. In these studies, the coupling was implemented for ad hoc applications, and we are currently in the process of coupling ROMS to RegCM4 for more general purposes.

2.3.2. Aerosols and chemistry

An area where substantial development has occurred in the last several years is the coupling with aerosols and atmospheric chemistry. A simplified aerosol scheme specifically designed for application to long-term climate simulations has been incrementally developed within the RegCM system. Solmon et al. (2006) first implemented a first-generation aerosol model including SO_2, sulfates, organic carbon, and black carbon. Zakey et al. (2006) then added a 4-bin desert dust module, and Zakey et al. (2008) implemented a 2-bin sea salt scheme. Additionally in RegCM4, the dust emission scheme accounts for sub-grid emissions by different types of soil, and the soil texture distribution has been updated according to Laurent et al. (2008). The dust emission size distribution can now also be treated according to Kok (2011). When all aerosols are simulated, 12 additional prognostic equations are solved in RegCM4, including transport by resolvable scale winds, turbulence and deep convection, sources, and wet and dry removal processes. As mentioned in Section 2.2.1, the aerosols are radiatively interactive both in the solar and infrared regions of the radiation spectrum. Various versions of this aerosol scheme were used to simulate the regional climatic effects of sulfate aerosols in China (Giorgi et al. 2002), Saharan dust (Konare et al. 2008, Solmon et al. 2008), Asian and Mediterranean dust (Zhang et al. 2009, Santese et al. 2010), and African biomass burning aerosol (Tummon et al. 2010, Malavelle et al. 2011).

The most recent addition to RegCM4 is in the area of gas-phase chemistry. A. Shalaby et al. (unpubl.) coupled to RegCM3 a set of gas-phase chemistry mechanisms of different complexity, the carbon-bond mechanism CBM-Z (Zaveri & Peters 1999), an extended version of the GEOS-Chem mechanism, and the comprehensive RADM2, with 2 numerical solvers, the Rosenbrock solver and a fast solver based on radical balance. These modules were tested by A. Shalaby et al. (unpubl.) in the simulation of the extreme ozone event of the summer 2003 over Europe. They showed that the combination of the CBM-Z, which treats 52 species for 132 reactions and requires the inclusion of 24 new prognostic tracers, along with the radical balance solver, provided the most computationally efficient simulation with a good representation of tropospheric chemistry. The chemistry solver is completed by a dry deposition scheme adapted from Zhang et al. (2003) and an emission preprocessing interface able to handle different emission inventories from the Global Emission Inventory Activity. When the CLM land surface scheme is activated, biogenic emissions can be calculated online using the MEGAN module (Guenther et al. 2006).

2.3.3. Tropical band configuration

A significant development of RegCM4 is the implementation of a tropical band configuration of the model. In this configuration, the model uses a Mercator projection centered over the equator for a band covering the entire tropical region, from 45° S to 45° N. The use of the Mercator projection allows the model grid to exactly cover the tropical band with the end points in the longitudinal direction exactly overlapping. This configuration requires the use of periodic boundary conditions in the longitudinal directions and the standard relaxation conditions at the northern and southern boundaries. In this way, information from the driving models is effectively provided only at these 2 boundaries. A test of this configuration, which offers many new applications, is presented by Coppola et al. (2012).

2.4. Computational aspects

A fundamental development in RegCM4 compared to its predecessors concerns its computational aspects. Essentially, the RegCM3 code has been largely rewritten to make it more flexible, user friendly, and portable on different computing architectures. More specifically, the code was made compliant to the ANSI F90 standard language, portability was enhanced with respect to compilers and computing platforms, and a single makefile for the entire system, from pre-processing to model code and post-processing, was implemented with a configure script that greatly simplifies the use of the model. In addition, modularity and multi-tasking for the code were substantially enhanced. With these implementations, the code can effectively run, depending on the domain size, on a large variety of high-performance computing platforms using up to several hundred processors.

3. EXAMPLES OF MODEL BEHAVIOR AND SENSITIVITIES

3.1. Experiments and analysis metrics

In order to provide illustrative examples of the model behavior and sensitivities, here we present a series of experiments with RegCM4 run over 4 different domains identified within the CORDEX framework. We first stress that we do not intend to provide a comprehensive and detailed analysis of the model performance but rather more simply an illustration of its basic behavior in different climatic settings. The selected domains are shown in Fig. 1, and include the European (EU), African (AFR), South American (SAM), and East Asian (EAS) CORDEX domains. Although the model is being tested for other domains as well, the choice of these specific domains for the present study was made because (1) they represent different climatic settings and (2) no other study

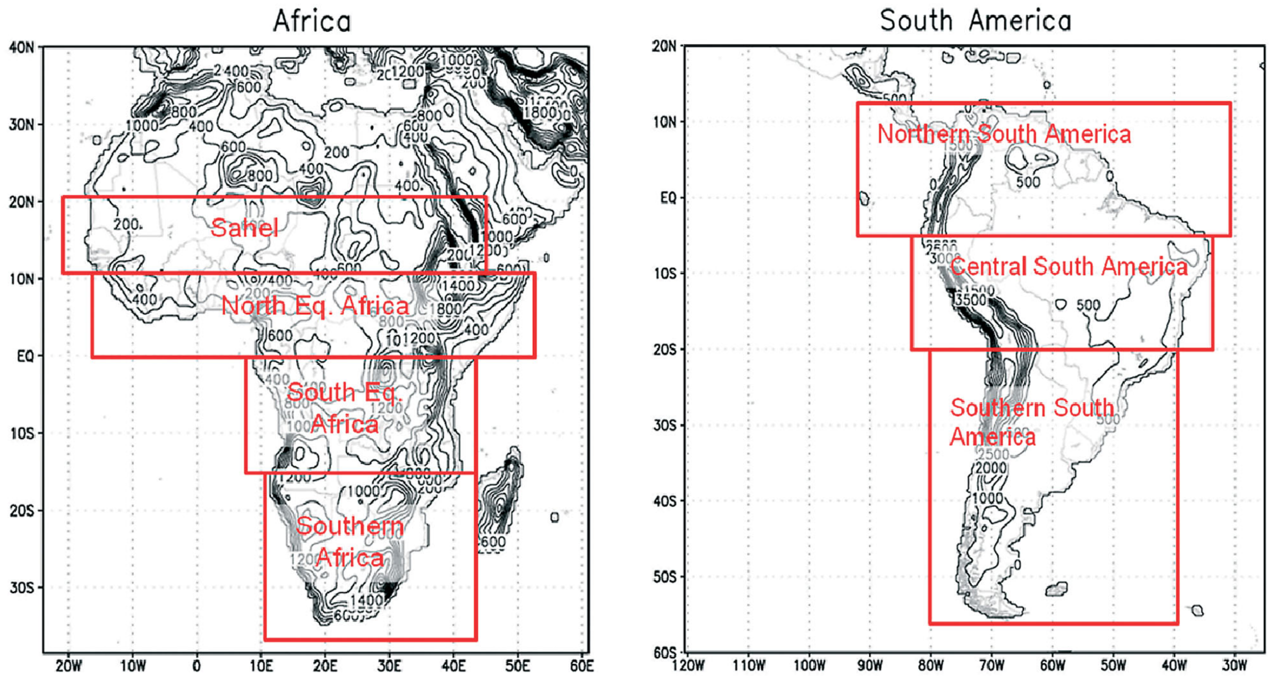

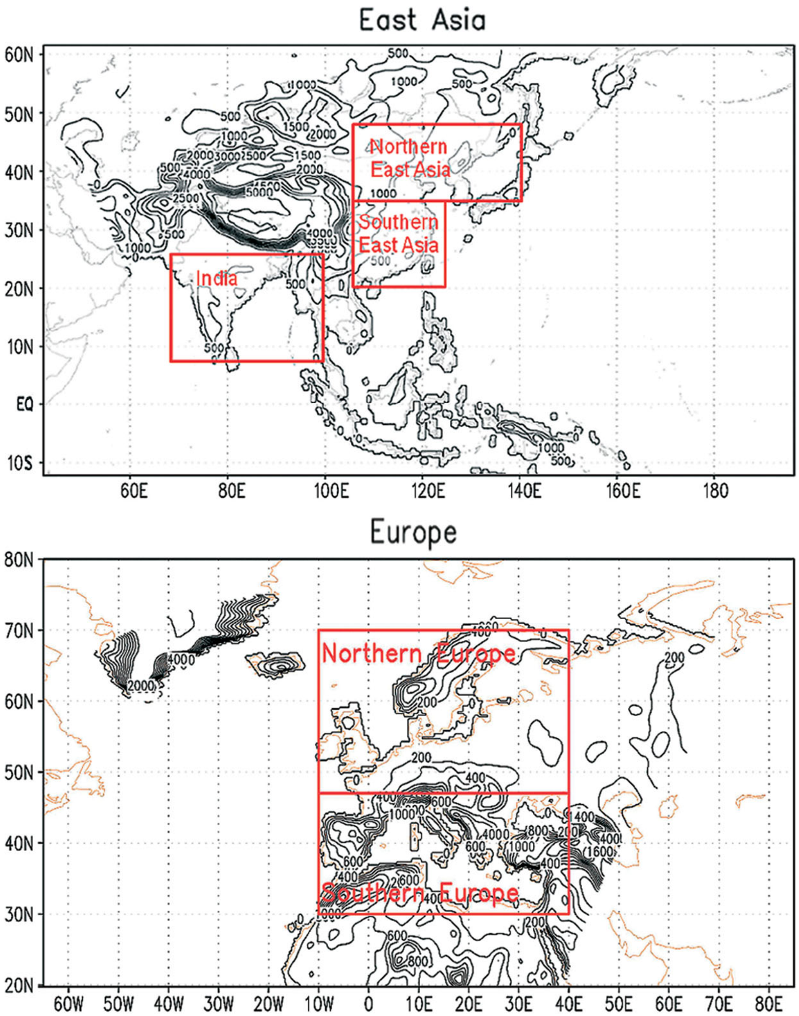

Fig. 1. Domain and topography (m) for the 4 domains used in this study. Also shown are sub-regions selected for more detailed analysis

in this Special issue focuses on these domains with RegCM4. The model grid spacing is 50 km, as specified in CORDEX, and the projection is Lambert conformal for the EU and EAS domains and rotated Mercator for the AFR and SAM domains. As in previous applications, the model employs 18 vertical sigma levels, with a model top at 50 hPa. For each domain, Fig. 1 also shows a set of sub-regions used for more detailed analysis.

For each domain, we performed and analyzed one or more 5 yr simulations (after discarding a 1 yr spin-up period) extending from 1 January 1998 to 31 December 2002, with lateral meteorological boundary conditions provided by the ERA-Interim reanalysis of observations, which has been shown to provide a much improved description of hydrologic cycle variables compared to previous products, especially over tropical regions (Uppala et al. 2008). Although 5 yr is not a long simulation time in order to produce robust statistics, the use of reanalysis boundary conditions allows us to compare the model results with actual observations for those specific 5 yr, thereby providing us with sufficient data for a first-order illustration of the model performance. The choice of this specific 5 yr period is tied to the availability of observations from the Tropical Rainfall Measuring Mission (TRMM; Huffman et al. 2007), which is an additional dataset used for model validation over tropical regions. The lateral buffer zone has a width of 15 grid points in each domain except for the EU one, where it is 12 grid points, and the exponential relaxation procedure described by Giorgi et al. (1993b) is used to provide the model with lateral boundary conditions.

Our illustrative analysis is mostly limited to precipitation, a key variable for impact assessment studies and an integrator of climate processes; however, some performance metrics are also calculated for temperature, and reference is made to previous or companion papers concerning other variables. The following datasets are used for model assessment: the TRMM (Huffman et al. 2007), which is available for both land and ocean areas and includes only precipitation; the station-based land dataset from the Climatic Research Unit of the University of East Anglia (CRU; New et al. 2000), which includes both surface air temperature and precipitation, and the CMAP precipitation dataset (Huffman et al. 1997), which is mostly used to complement the CRU data over ocean areas.

For all domains, the model is run in its mixed convection configuration as baseline, which employs the Grell scheme over land and the MIT scheme over ocean. An extensive set of preliminary experiments showed that overall this configuration provides the best results over most domains, particularly over tropical regions. In this regard, our RegCM4 experiments are significantly different from previous RegCM3 experiments that utilized only one scheme. Of the new features, all runs use the diurnal SST scheme, fractional clear sky radiation calculations, and modified Holtslag PBL diffusivity in very stable conditions. The model configuration is the same in all domains except for the setting of key parameters in the Grell convection scheme (maximum and minimum Peff), SUBEX resolvable scale precipitation scheme (Cevap and Qth), and BATS land surface parameterization (minimum stomatal resistance, or rsmin). In this latter case, while the original BATS formulation employed a value of rsmin of 200 s m^{-1} for all land types, Pal et al. (2007) introduced lower values in the range of 50 to 100 s m^{-1}. In preliminary experiments, we found that these lower values led to excessively high evaporation amounts and precipitation feedbacks, so that in RegCM4 we went back to the original BATS formulation.

Although these values represent only a very small subset of the full parameters present in the model, they were found to provide a substantial model sensitivity in preliminary experiments. The parameter values tested here are reported in Table 2. For the smaller EU domain, we completed, and discuss, a set of experiments with multiple options (see Table 2), in particular one including the UW-PBL scheme (T. A. O'Brien et al. unpubl.). For the SAM domain, we discuss 2 sensitivity experiments (Table 2), while for the AFR and EAS domains we completed only 1 experiment.

In this paper, we use 3 evaluation metrics: the mean absolute bias (MAB, the mean of the grid point absolute bias averaged over a given region), the mean bias (BIAS), and the pattern correlation coefficient (COR). The MAB and COR provide information on the model performance at the grid point level, and are thus stringent tests of model performance, while the BIAS provides information at the regional or subregional level and is thus a measure of systematic model errors. These metrics are calculated for each of the subregions indicated in Fig. 1 and for the main continental areas in the domain. The analysis is per-

Table 2. Set of sensitivity experiments analyzed in this paper. Cevap: rate of sub-cloud evaporation; Peff: fraction of precipitation evaporated in the downdraft (i.e. 1 – precipitation efficiency); Qth: in-cloud liquid water threshold for the activation of the autoconversion term; rsmin: minimum stomatal resistance

Domain	Experiment
Africa	Baseline (Cevap = 1.0×10^{-3}, $\text{Peff}_{min} = 0.25$, $\text{Peff}_{max} = 1.0$)
South America	DRY ($\text{Peff}_{min} = 0.25$, $\text{Peff}_{max} = 1.0$) WET ($\text{Peff}_{min} = 0.25$, $\text{Peff}_{max} = 0.5$)
East Asia	Baseline (same as for Africa)
Europe	Expt 1 (Cevap = 2.0×10^{-4}, $\text{Peff}_{min} = 0.25$, $\text{Peff}_{max} = 1.0$, increased Qth) Expt 2 (As Expt 1 but Grell scheme over ocean) Expt 3 (As Expt 1 but MIT scheme over land) Expt 4 (As Expt 2 but Cevap = 1×10^{-3}) Expt 5 (As Expt 2 but UW-PBL scheme) Expt 6 (As Expt 2 but reduced rsmin from Pal et al. 2007)

formed for the 6 mo long seasons April through September (A–S) and October through March (O–M), so that the entire year is considered. For each sub-region, we also examine the annual cycle of both temperature and precipitation.

The performance metrics are all calculated with respect to the CRU observations both because these observations are available for all domains and the full period and because the resolution of these data best matches the model resolution. On the other hand, it should be recognized that different datasets can show substantial differences (see Sections 3.2–3.5), especially over tropical regions, and therefore the performance metrics values should be considered only as indicative in view of this uncertainty.

3.2. AFR domain

We begin with the AFR domain, the priority domain within the CORDEX program (Giorgi et al. 2009). For this domain, the largest considered here, we completed 1 full simulation (Table 1). Fig. 2 intercompares A–S and O–M precipitation and low level wind (850 HPa) across 2 observational datasets (CRU+CMAP and TRMM) and the RegCM4 simulation. Corresponding biases over land areas with respect to the CRU observations are also shown. The model clearly captures the basic observed patterns of both mean precipitation and low level circulation. The Intertropical Convergence Zone (ITCZ) over the Atlantic is somewhat narrower in the model than in the observational products, but the regional features of the precipitation field are well reproduced in both seasons, as are the main monsoon flow characteristics. This result is consistent with the previous version of the model (Sylla et al. 2010), and, as in this previous version, RegCM4 captures the basic features of prominent upper level circulations such as the Tropical Easterly Jet and the African Easterly Jet (not shown for brevity). An analysis of the bias values reveals the main deficiencies in the present run. Precipitation is overestimated over the west and east African monsoon region in A–S and over the Lake Victoria and southeastern African areas in O–M. Conversely, the model is too dry over the lower Congo Basin.

Fig. 3 shows the surface air temperature and precipitation annual cycles over the 4 African sub-regions of Fig. 1. This figure shows that over the Sahel region, most of the precipitation overestimate occurs in the spring pre-monsoon season (April to June), while during the mature and receding monsoon phases, the agreement with observations is excellent. Sylla et al. (2010) overestimated precipitation throughout the entire monsoon season, especially over eastern Africa. RegCM4 appears to correct the overestimate from July to September, but still maintains this bias in the pre-monsoon season.

Over north equatorial Africa, the model agrees well with observations, showing a double rainy season related to the latitudinal migration of the ITCZ and related monsoon rain. This double rainy season indeed appears even more pronounced than in the observational products, probably as a result of the sharper definition of the monsoon rain band in the model. Finally, over both the south equatorial african and South African regions, the model reproduces well the annual cycle of precipitation. Concerning the annual temperature cycles (Fig. 3), the model shows a very good agreement with observations in all regions, with biases at the monthly scale mostly close to or less than 1°C.

Table 3 reports the MAB, BIAS, and COR values for temperature and precipitation over the 4 African sub-regions and the entire African continent. The temperature metrics confirm the excellent agreement with observations, with correlations exceeding 0.85, MAB less than 1.2°C, and biases less than 1°C for both seasons. A more varied performance is found for precipitation. The pattern correlation is about 0.7 or greater in all sub-regions (>0.8 for the whole African continent), except for south equatorial africa, where it is low especially in O–M. Biases are less than 20 % in all sub-regions (less than 10 % for the continent) except for the Sahel in A–S, where precipitation is overestimated by about 32 % (mostly due to the spring months, as seen above), and over south equatorial Africa in O–M (underestimate of about 36 %). The MAB is between 36 and 62 % (~40 to 45 % for the entire African continent).

The metrics in Table 3 should be interpreted with caution. These metrics are calculated with respect to the CRU dataset and rely heavily on the spatial distribution of these observations down to the grid point level (for the MAB and COR). However, a large uncertainty is present in the observations, particularly in remote areas were the precipitation field is often interpolated from a sparse distribution of available stations. This uncertainty would therefore most affect metrics based on high-resolution information.

As a summary assessment, the overall performance of the model over the AFR domain appears improved compared to Sylla et al. (2010), with the noticeable exception of excess rainfall in the premonsoon sea-

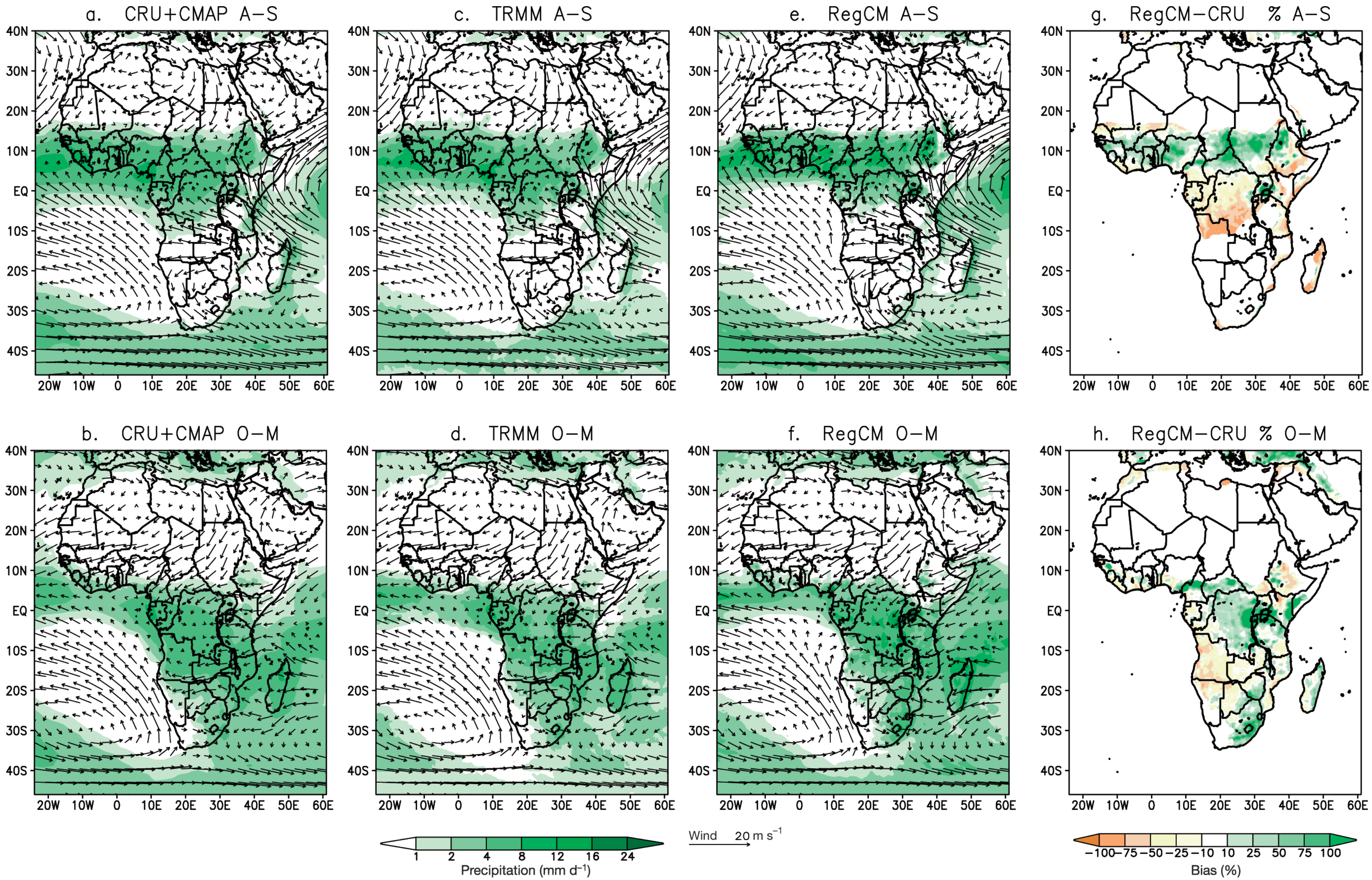

Fig. 2. Mean precipitation and low level wind over the African domain in the (a,b) CRU+CMAP and (c,d) TRMM observations, as well as (e,f) RegCM4 simulation. (g,h) Mean bias between simulated and observed CRU precipitation. (a,c,g,e) April to September (A–S), (b,d,f,h) October to March (O–M). In (a) and (b), CRU observations are used over land and CMAP observations over ocean. Observed winds are taken from the ERA-Interim reanalysis

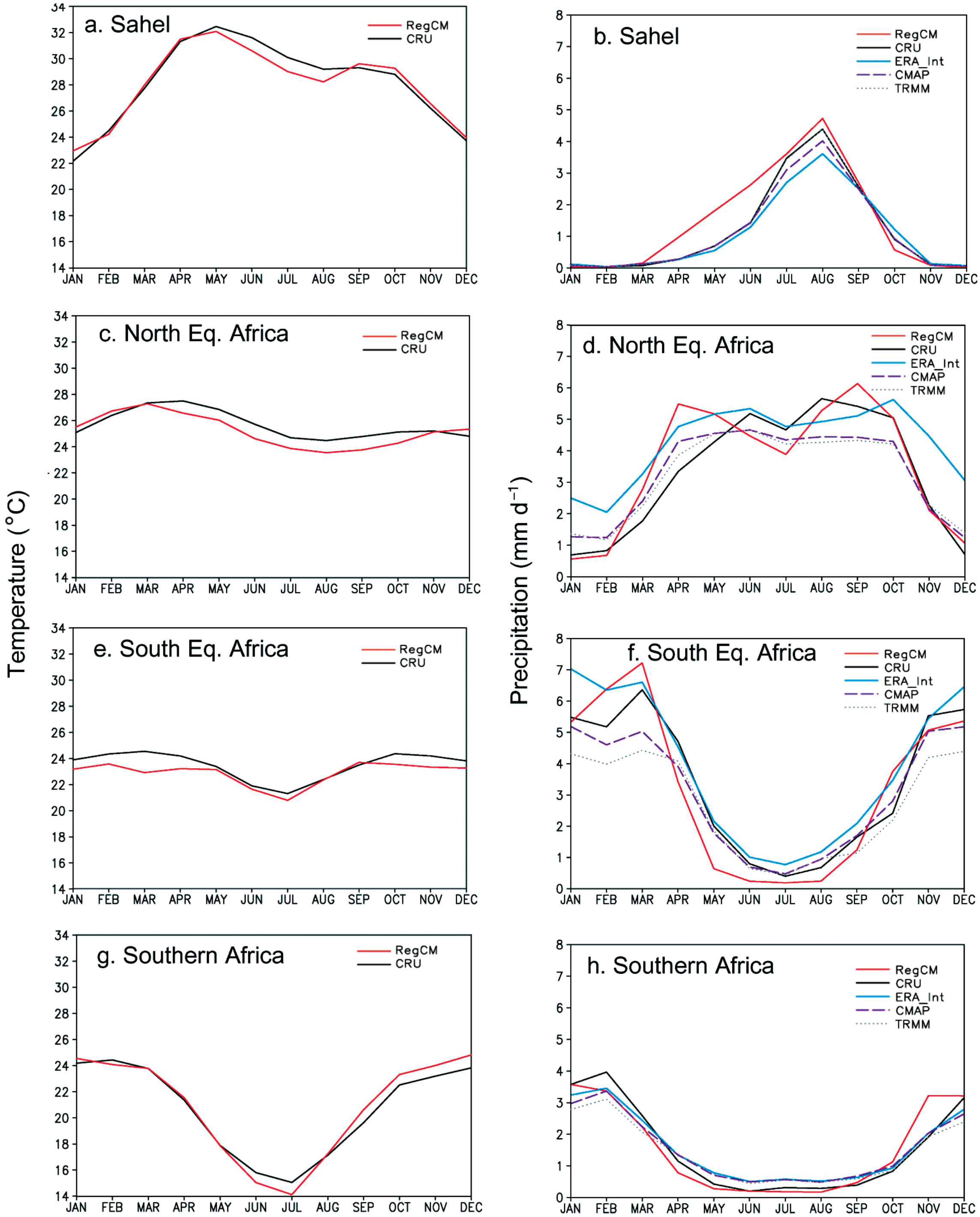

Fig. 3. Annual cycles of observed and simulated temperature and precipitation over the 4 African sub-regions shown in Fig. 1

son over the Sahel region. We are currently conducting some sensitivity experiments to assess the origins of this bias, for which, for example the lack of dust effects (Konare et al. 2008, Solmon et al. 2008) or the land surface conditions (Abiodun et al. 2008), might also be relevant contributors.

3.3. SAM domain

For the SAM domain, we conducted 2 simulations in which the parameter settings of the Grell scheme led to what we call WET and DRY configurations (Table 2). Fig. 4 intercompares simulated and observed A–S and O–M mean precipitation and low level wind patterns for the DRY case. Again, a general agreement across all fields is found both over land and ocean areas. The model appears to somewhat underestimate the low level southerly jet in A–S, which leads to an underestimate of precipitation over the La Plata and lower Amazon basin (Fig. 4g,h). In fact, for this DRY case a general underestimate of precipitation prevails over the Amazon Basin, which is much reduced in the WET case. On the other hand, over the coastal regions of northeastern Brazil, precipitation is much better simulated in the DRY than the WET case, which substantially overestimated it.

Fig. 5 shows the observed and simulated annual cycle of precipitation and temperature, where both the DRY and WET cases are included. Over northern South America, the model reproduces the observed annual cycle of precipitation. However, the WET case substantially overestimates precipitation throughout the year, while the DRY case lies within the range of the observational data. We note that the observations themselves show a large uncertainty, with CRU values being much larger than CMAP and TRMM, so that the dry bias in Fig. 5g,h may actually be artificially amplified by the use of the CRU observations as reference. Over the central South American region, again the annual cycle of precipitation is well captured, but the DRY case underestimates precipitation, while the WET case is within the observational uncertainty. Finally, both the WET and DRY cases agree well with observations over the southern South American region, where the model sensitivity to the convection parameters appears relatively small.

The temperature annual cycle (Fig. 5a,b) is weak in the northern South American region, which lies mostly close to the equatorial belt, and becomes increasingly pronounced in the central and southern South American regions. The model shows a systematic cold bias of around 2°C in both the northern and central South American regions, slightly greater in the December–January–February (DJF) than in the June–July–August (JJA) periods. This results in an underestima-

Table 3. Precipitation (%) and surface air temperature (°C) mean absolute bias (MAB), mean bias (BIAS), and pattern correlation coefficient (COR) over different regions in illustrative experiments (see Section 3 for details). A–S: April–September; O–M: October–March

	MAB		BIAS		COR	
	A–S	O–M	A–S	O–M	A–S	O–M
Africa (Baseline)						
Precipitation						
Sahel	50.2	62.3	32.2	−17.8	0.88	0.74
North equatorial	34.3	41.2	7.1	16.7	0.71	0.69
South equatorial	56.1	39.0	−35.8	12.4	0.53	0.10
South Africa	50.3	36.3	−14.9	−0.3	0.70	0.72
Whole	44.6	39.9	2.7	9.2	0.85	0.81
Temperature						
Sahel	1.02	0.87	−0.55	0.29	0.94	0.92
North equatorial	1.14	0.86	−0.87	0.02	0.89	0.92
South equatorial	1.22	1.14	−0.23	−0.82	0.89	0.85
South Africa	1.09	1.04	0.03	0.22	0.89	0.90
Whole	1.20	0.99	−0.30	−0.23	0.95	0.97
South America (DRY)						
Precipitation						
Northern	34.1	36.2	−10.7	3.9	0.37	0.31
Central	40.5	36.1	−32.9	−25.5	0.86	0.62
Southern	45.9	35.9	−4.7	16.5	0.69	0.75
Whole	37.5	36.1	−14.5	−7.6	0.79	0.55
Temperature						
Northern	3.21	2.92	−2.98	−2.71	0.78	0.82
Central	1.31	2.05	−0.51	−1.86	0.95	0.96
Southern	1.94	1.52	−1.56	−0.41	0.97	0.95
Whole	2.06	2.14	−1.57	−1.67	0.96	0.94
East Asia (Baseline)						
Precipitation						
Northern	25.0	84.7	10.5	80.0	0.81	0.91
Southern	18.0	30.8	−9.7	−6.7	0.42	0.62
India	40.3	51.7	−14.3	4.3	0.65	0.54
Temperature						
Northern	0.74	2.03	−0.36	−0.95	0.96	0.94
Southern	0.79	2.66	0.04	−2.44	0.89	0.97
India	1.58	1.71	−0.10	−1.45	0.89	0.90
Europe (Expt 1)						
Precipitation						
Northern	39.3	30.6	−1.6	−5.8	0.79	0.80
Southern	21.0	31.0	−5.6	0.7	0.46	0.66
Whole	27.7	30.8	−4.15	−2.3	0.78	0.71
Temperature						
Northern	1.20	1.37	−0.06	−0.20	0.94	0.94
Southern	0.83	1.40	0.54	−1.27	0.98	0.97
Whole	1.02	1.38	−0.23	−0.51	0.97	0.98

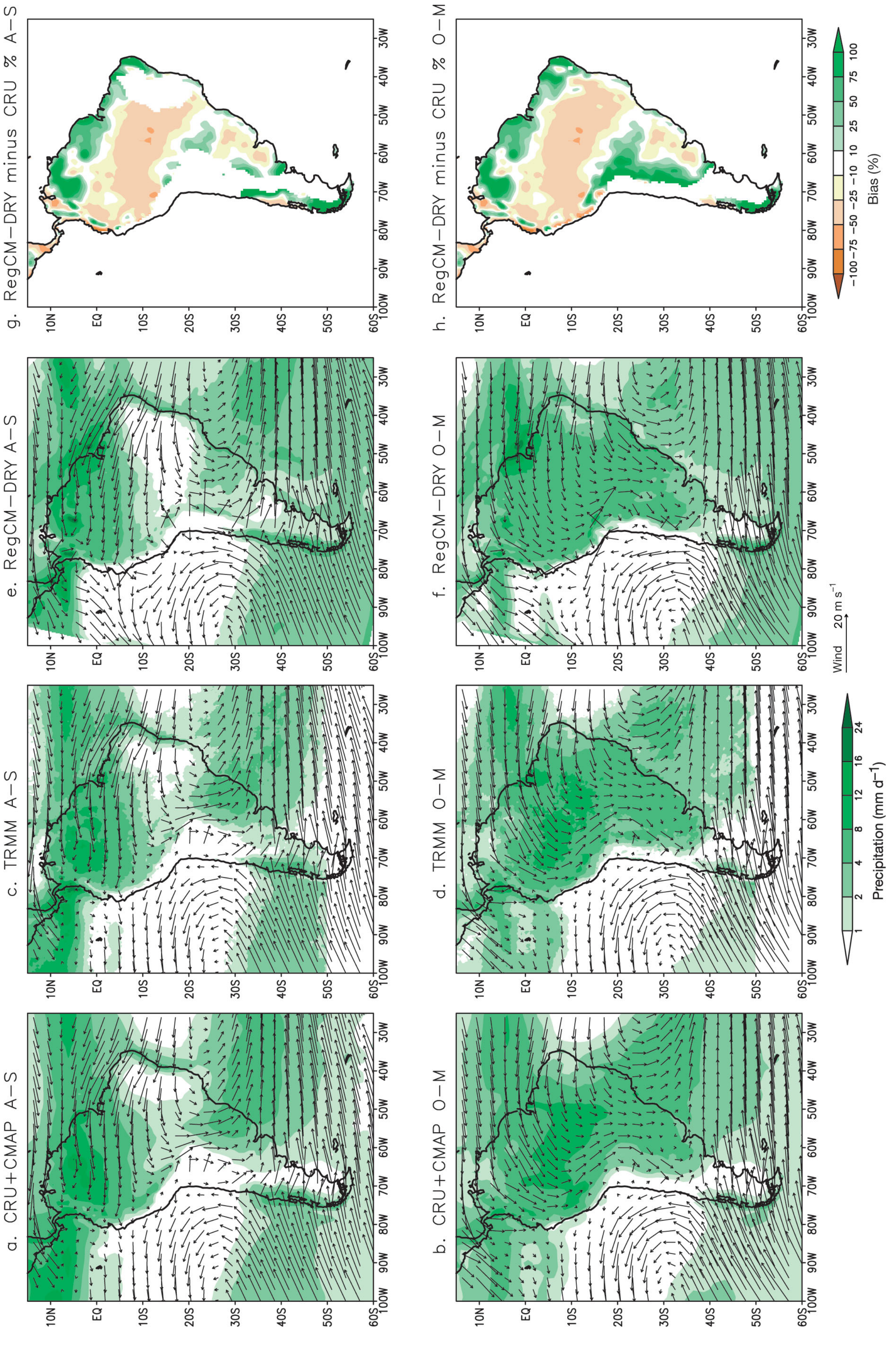

Fig. 4. Mean precipitation and low level wind over the South American domain. Details as in Fig. 2

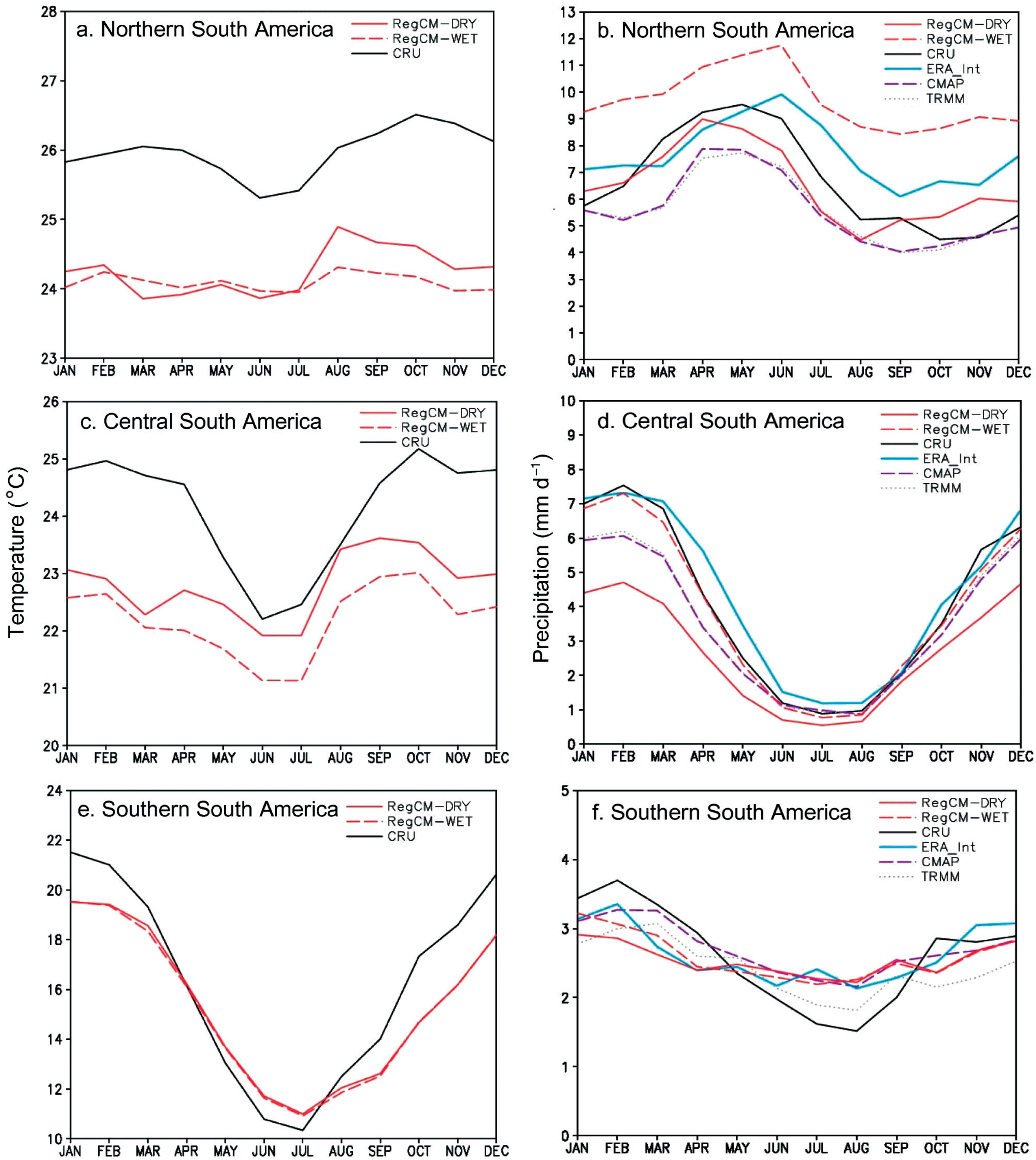

Fig. 5. Annual cycles of observed and simulated temperature and precipitation over the South American domain

tion of the seasonal temperature cycle, which is also found in the southernmost region. In fact, in this latter region the RegCM4 shows a cold bias in DJF but a warm bias in June and July.

Table 3 shows the 3 performance metrics calculated for the South American regions in the DRY case. As for the African region, the pattern correlation coefficients are mostly high, >0.78 for temperature and >0.55 for precipitation, with the noticeable exception of the northern South American region, where they are in the range of 0.31 to 0.37. The temperature BIAS and MAB values are generally higher than for Africa, again in particular over the northern region, while the precipitation metrics have comparable values. In particular, the MAB is between 35 and 45 % and the dry bias in the Central South America region is evident from the BIAS metric. The wet case (not shown for brevity) showed metrics of similar magnitude except large positive biases in excess of 45 % over northern South America.

Overall, although the model exhibits a reasonably good performance over the SAM domain, some significant systematic biases are found, both for precipitation and temperature. Previous applications of the RegCM to this region have shown varied levels of performance (e.g. da Rocha et al. 2009). In addition, similarly to the case of Africa, the observational data are likely affected by significant uncertainties, particularly in remote areas of the Amazon basin, and this makes a rigorous model assessment over this region rather difficult. Moreover, the surface climate of the Amazon basin is influenced by local processes involving land–atmosphere interactions (Koster et al. 2004), so that the treatment of surface processes is crucial. In this regard, further testing is underway to assess the sensitivity of the model to land surface schemes and parameter specification over this domain.

3.4. EAS domain

One test experiment was performed over the EAS domain (Table 2). Traditionally, the RegCM system has shown some systematic biases over this region, particularly in the winter season such as a cold bias over southeastern China, a warm bias over the northernmost areas of the Asian continent, and an overestimate of precipitation (Gao et al. 2001). Conversely, the simulation of summer monsoon climate has shown a good agreement with observations (Gao et al. 2008) and a substantial dependency on model resolution (Gao et al. 2006). Note that the Indian continent is also included in this CORDEX domain, and it is thus presented in this analysis for illustrative purposes. However, we note that India lies close to one of the domain boundaries and that another CORDEX domain actually focuses on the South Asian region (Giorgi et al. 2009).

Comparison of simulated and observed precipitation is presented in Fig. 6 (along with low level winds) and Fig. 7 (annual cycle for the 3 sub-regions of Fig. 1). Similarly to other regional domains, the basic patterns of mean precipitation and low level circulation are generally captured. In all regions, the seasonal evolution of monsoon precipitation is well reproduced, with main errors being an overestimate of precipitation in spring over the northern East Asian region and an underestimate of peak monsoon precipitation during the mature phase in the southern East Asian and Indian sub-regions. The temperature annual cycle is generally well reproduced over the 3 regions analyzed, except for the winter months over the southern East Asian and, to a lesser extent, the Indian domains, where a cold systematic bias of a few degrees remains.

The performance metrics over the EAS domain sub-regions are reported in Table 3. The values are mostly in line with the previous 2 domains, with noticeable cases of large systematic errors being the winter cold bias over southern East Asia (–2.4°C) and the large overestimation of cold season precipitation over northern East Asia, which may be amplified by the low reference precipitation there during this season. We also note that the model performance metrics over the Indian region are of the same quality as, or even better than, those of the other regions, even though this area lies close to the western boundary of the domain and is not the focus of this domain. In this regard, we find a dry bias over the northern Indian regions, which was not found in analogous simulations for the corresponding South Asian CORDEX domain.

3.5. EU domain

A number of sensitivity experiments were carried out for the EU domain, the smallest of the set analyzed here (Table 1). These sample different values of resolvable scale precipitation and evapotranspiration parameters. Previous versions of the model, which participated in a series of EU projects (e.g. PRUDENCE and ENSEMBLES) were characterized by a persistent cold bias in the winter season (Giorgi et al. 2004) and a general overestimate of precipitation, particularly in the winter (Rauscher et al. 2010). For this reason, in all experiments we employed increased values of Qth compared to the other domains by a factor of 2. The set of parameterizations and parameter settings shown here is actually an illustrative sub-set of a broader set of test experiments performed for this domain. Note that for comparison purposes in the UW-PBL experiment we use the same number of vertical levels as in the default version (18); however, this parameterization usually requires a higher number of levels in the PBL (T. A. O'Brien et al. unpubl.).

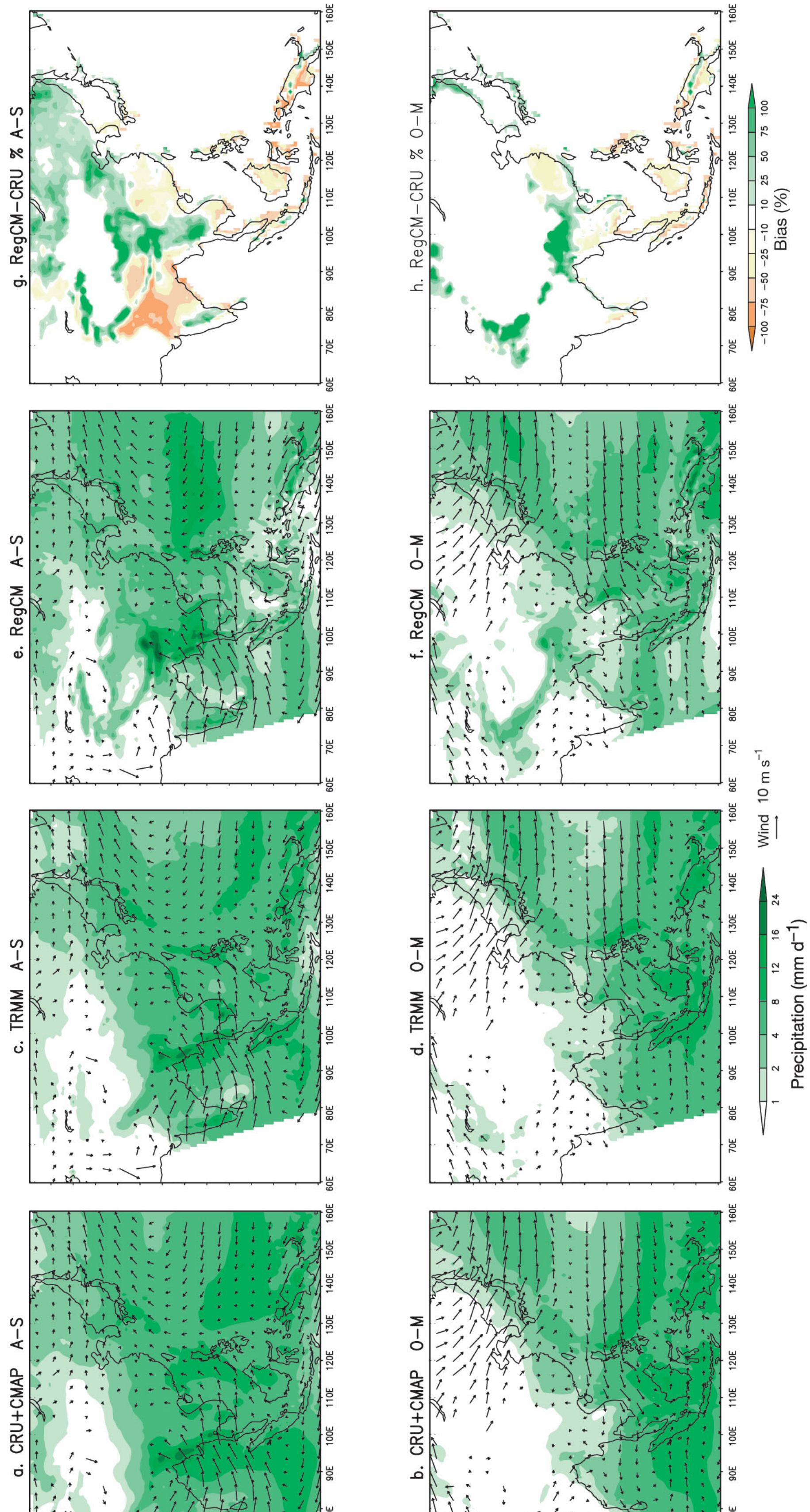

Fig. 6. Mean precipitation and low level wind over the East Asian domain. Details as in Fig. 2

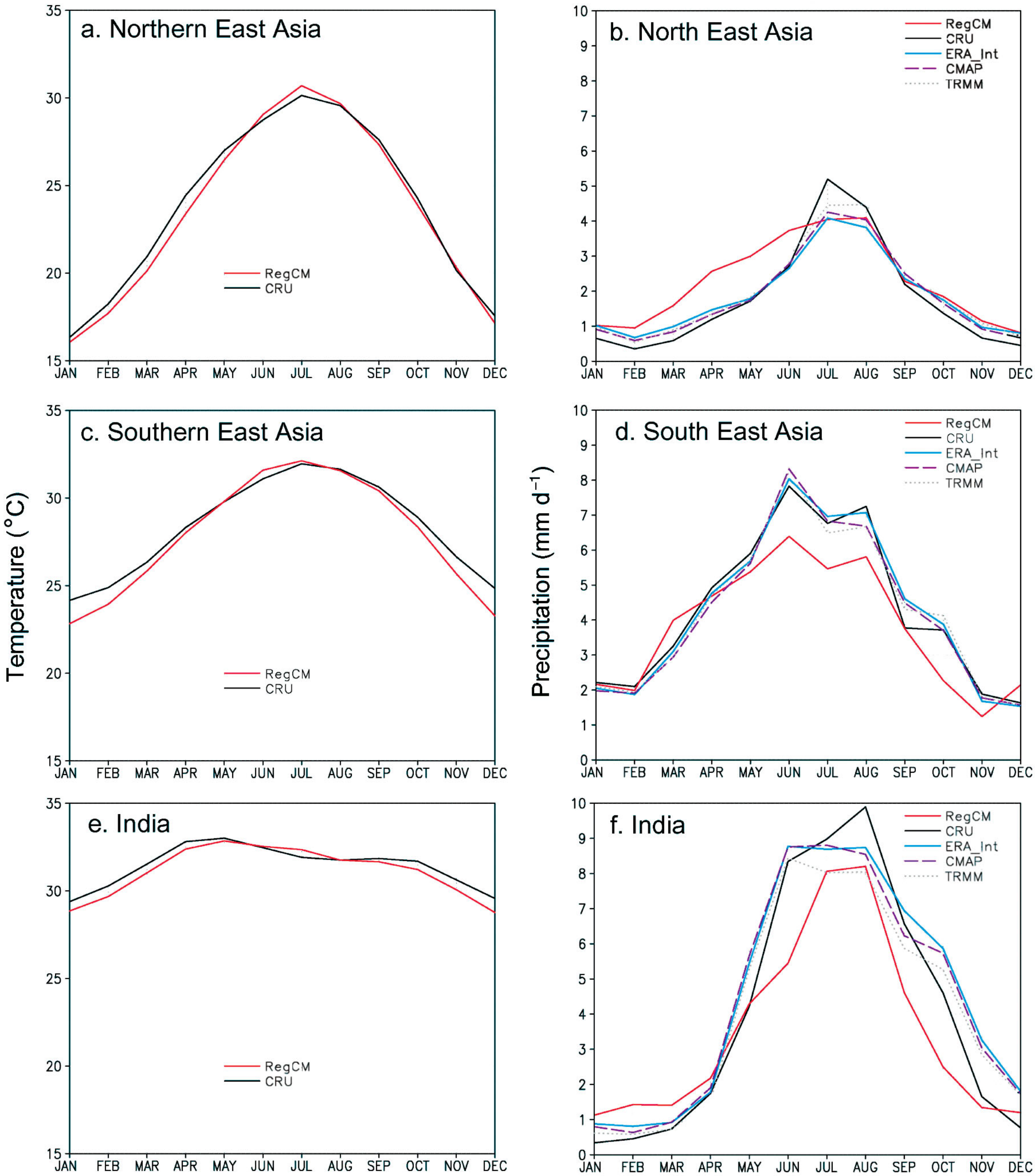

Fig. 7. Annual cycles of observed and simulated temperature and precipitation over the East Asian domain

Fig. 8 first compares observed and simulated mean precipitation and low level wind circulations, along with corresponding biases, for the 'baseline' experiment employing the mixed MIT-Ocean / Grell-Land configuration. This was in fact the best performing experiment of the set. Precipitation and circulations are well reproduced, and large areas of the domain show relatively small precipitation biases (less than 10 %). Among the most prominent biases, we found a precipitation overestimate in the cold season over central eastern Europe and a dry bias during the warm portion of the year over southeastern Europe. The latter has been a consistent feature of a number of regional models for the European region (Jacob et al. 2007, Rauscher et al. 2010).

Annual cycles of temperature and precipitation over the northern and southern European regions are shown in Fig. 9. The temperature annual cycle is well

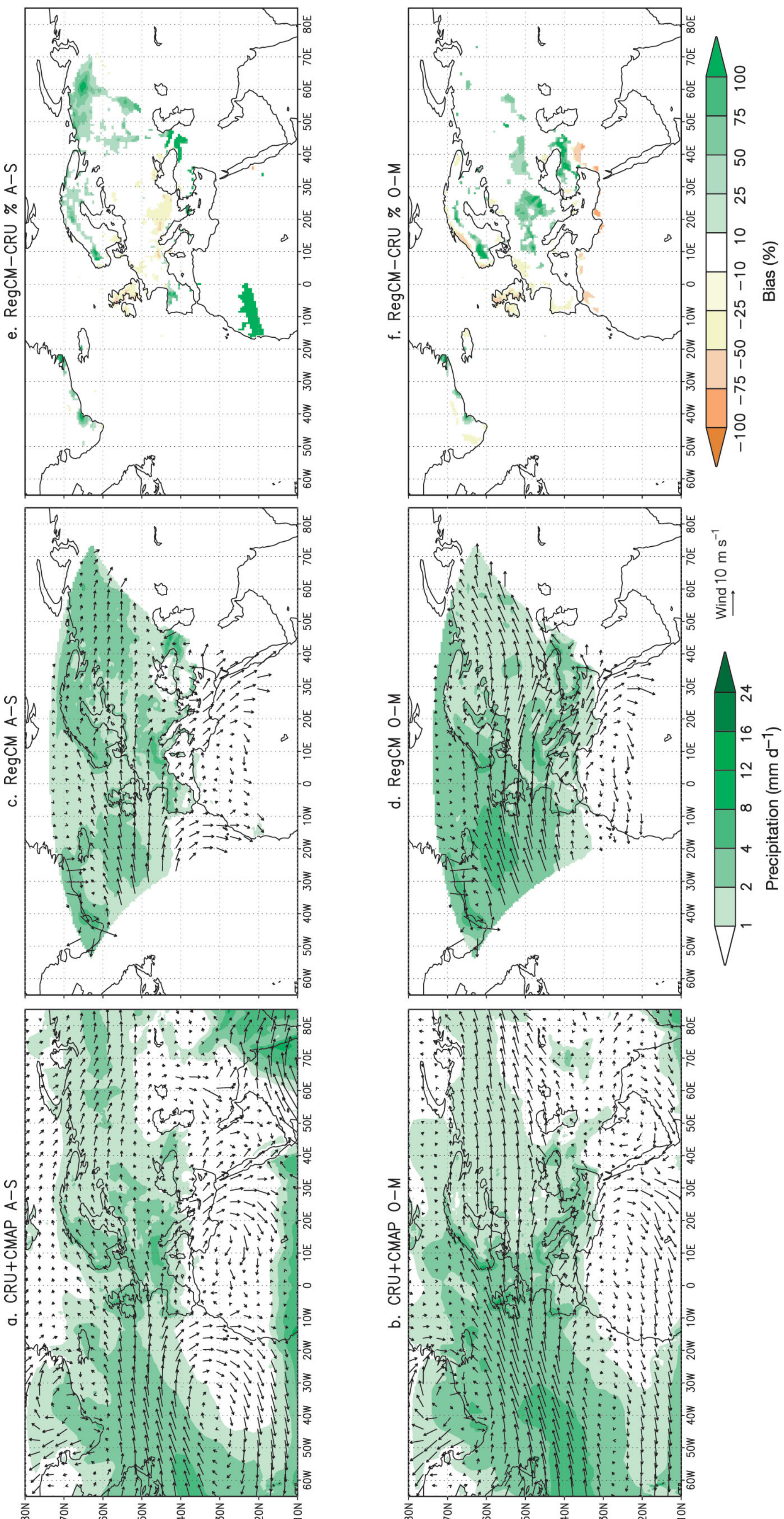

Fig. 8. Mean precipitation and low level wind over the European domain. Details as in Fig. 2

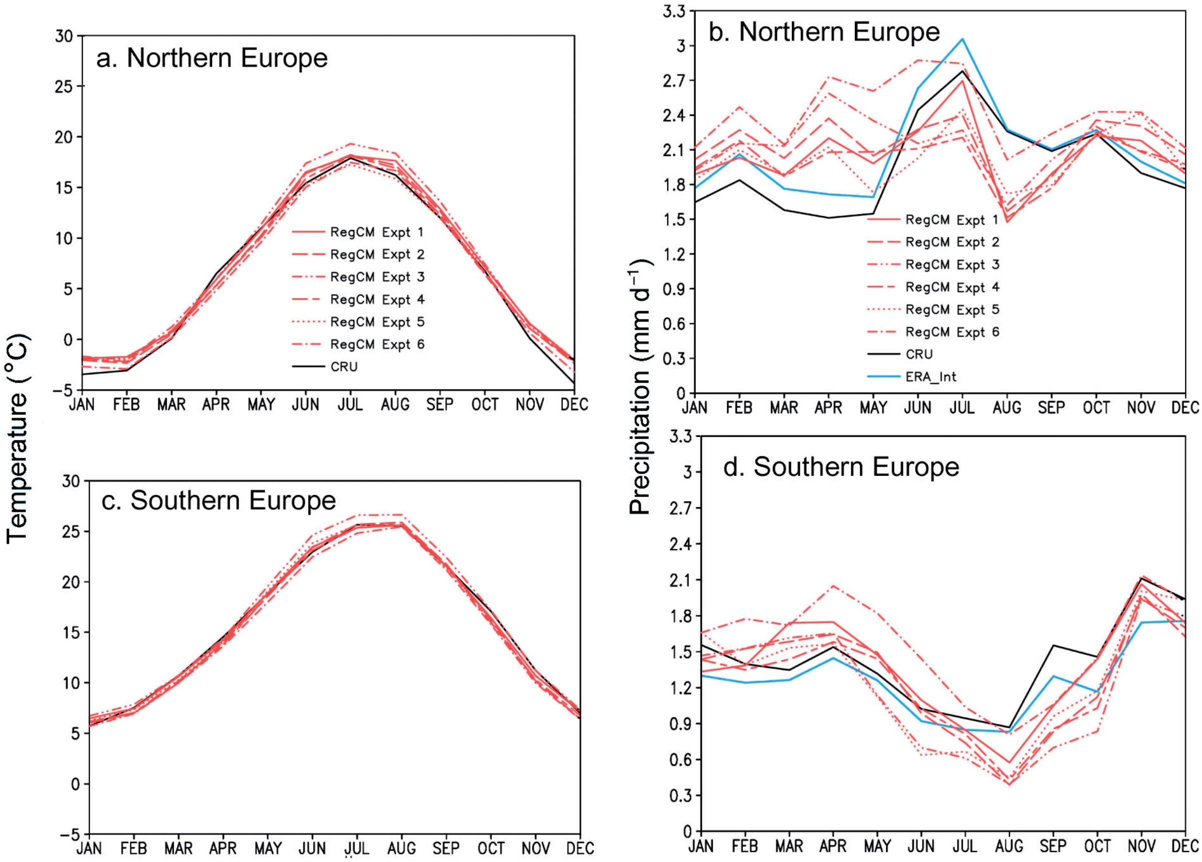

Fig. 9. Annual cycles of observed and simulated temperature and precipitation over the European domain

reproduced in both regions. Precipitation is generally overestimated over northern Europe in the winter and spring months in all simulations. This result, which is consistent with previous applications of the model, is likely artificially amplified by the lack of a gauge undercatch correction in the CRU observations, which may lead to an underestimate in observed precipitation of up to 30% (Adam & Lettenmaier 2003). In the summer, more mixed results are found. Most sensitivity experiments underestimate precipitation throughout the summer, except for the baseline one, which actually shows a good agreement with observations in June and July over both regions, but a significant underestimate in August. Indeed, most experiments exhibit a dry bias in this month. As mentioned, most of this dry bias occurs over eastern and southeastern Europe. We also note that the effect of the UW-PBL scheme on precipitation is not large, as the annual cycle of precipitation in this experiment is generally in line with the others. A similar result was found for surface air temperature.

The largest sensitivity is found in the experiment in which the minimum stomatal resistance is decreased (Expt 6, see Table 2), pointing to strong land–atmosphere feedbacks in the model. In this latter case, precipitation is substantially overestimated in the spring over both southern and northern Europe, so that the soil moisture is high at the beginning of summer and the soil water–precipitation feedback leads to increased precipitation also in late summer. In Expt 6, although precipitation is better simulated in summer compared to the baseline run, it appears excessively overestimated in the other seasons.

We finally note that, although reduced compared to previous versions, the model still has a warm bias of up to several degrees in the coldest northeastern regions of the domain in winter (not shown), although part of it is inherited by the forcing ERA-Interim fields. It is likely that a much higher resolution in the boundary layer is needed to better capture low level inversions in very stable conditions.

Table 3 shows the performance metrics for the European baseline simulation. They are somewhat better than for the other regions, which does not necessarily imply a better model performance but could also be due to the better quality of the observed data. Regional temperature biases are mostly less than 1°C and MAB less than 1.5°C. Regional precipitation biases are also small, less than 10%, while the MAB values are in the range of 20 to 40%. Finally the pattern correlations are high (>0.65) both for temperature and precipitation, except for a lower value (0.46) for warm season precipitation over southern Europe. We also calculated the performance metrics for the other experiments, which were somewhat worse than, but not very distant from, those for the baseline case. As a summary assessment, the performance of RegCM4 over the European region appears in line with or better than previous versions of the model run at the same resolution.

4. CONCLUSIONS

In this paper, we have presented the newly released version of the RegCM regional climate modeling system, RegCM4. Compared to previous versions, it includes new parameterization schemes (the CLM land surface process scheme, the UW-PBL scheme, and the diurnal SST scheme), significant modifications of pre-existing schemes (the Holtslag PBL and the radiative transfer package), new model configurations (the mixed convection and tropical band capability), and a major code upgrade effort to make the model more clean, flexible, and portable on different compilers and computing architectures. Like the previous version, RegCM4 can be used in multiple 1-way nested mode, although 2-way nesting is still not available.

A series of tests and sensitivity experiments over 4 CORDEX domains (Giorgi et al. 2009) was presented to illustrate aspects of the model behavior and sensitivities in different climatic regimes. The model tends to show a consistent level of performance, as measured by simple aggregated metrics, across model domains, although some systematic model biases do persist. The model also shows a significant sensitivity to different parameterizations and parameter settings, which can thus be used to optimize the model performance over different domains. We stress that, although some model configuration characteristics appear to perform generally better over the majority of the domains (e.g. the mixed convection approach), there is no single parameter setting that performs best in all domains tested; therefore, we recommend conducting a customization exercise before carrying out specific model applications.

The present version of the model, named RegCM4.1, is presently frozen and available for community use (http://eforge.escience-lab.org/gf/project/regcm). Being a new version, it still requires testing, and we recommend that eventual users further assess the model sensitivities and provide us feedback on their findings. Such feedback has been instrumental in the past to improve not only the model performance but also the model portability. Several enhancements are currently underway. We are in the process of implementing the Tietdke convection scheme (Tiedtke 1989), and this option should be available for a release (RegCM4.2) planned for the end of 2011. This release is also scheduled to include coupling with the CBMZ chemical module with the Sillmann fast solver, the ROMS regional ocean model, and semi-Lagrangian advection for water vapor and chemical tracers.

In terms of applications, in coordination with the RegCNET community (Giorgi et al. 2006), we plan to use RegCM4 to produce climate change projections within the CORDEX framework for at least 6 domains: Africa, Europe, Central America, South America, East Asia, and South Asia. In addition, also as part of a series of European projects, we plan to use the model for studies of chemistry–climate interactions, land–atmosphere interactions, and climate impacts on hydrology, agriculture, and human health. Two areas that will constitute major developments are the implementation of a semi-Lagrangian, semi-implicit, finite volume element non-hydrostatic dynamical core and an improved cloud microphysics scheme accounting for cloud ice processes and interactions with atmospheric aerosols. These major changes will provide the basis for the next version of the RegCM modeling system, RegCM5. Over the long term, our modeling effort will continue to go towards the development of a fully coupled, flexible, and portable regional Earth System model applicable to a wide range of studies and available for public use by the broader scientific community.

Acknowledgements. We thank 3 anonymous reviewers for their useful comments, which helped to improve the quality of this paper.

LITERATURE CITED

Abiodun BJ, Pal JS, Afiesimama EA, Gutowski WJ, Adedoyin A (2008) Simulation of West African Monsoon using regCM3. II.Iimpacts of deforestation and desertification. Theor Appl Climatol 93:245–261

Adam JC, Lettenmaier DP (2003) Adjustment of global gridded precipitation for systematic bias. J Geophys Res 108: 4257, doi:10.1029/2002JD002499

Anthes RA (1977) A cumulus parameterization scheme utilizing a one-dimensional cloud model. Mon Weather Rev 105:1423–1438

Anthes RA, Hsie EY, Kuo YH (1987) Description of the Penn

State/NCAR Mesoscale Model Version 4 (MM4). National Center for Atmospheric Research Tech Note TN-282+STR, NCAR, Boulder, CO
Artale V, Calmanti S, Carillo A, Dell'Aquila A and others (2010) An atmosphere–ocean regional climate model for the Mediterranean area: assessment of a present climate simulation. Clim Dyn 35:721–740
Bretherton CS, McCaa JR, Grenier H (2004) A new parameterization for shallow cumulus convection and its application to marine subtropical cloud-topped boundary layers. I. Description and 1D results. Mon Weather Rev 132:864–882
Briegleb BP (1992) Delta-Eddington approximation for solar radiation in the NCAR Community Climate Model. J Geophys Res 97:7603–7612
Coppola E, Giorgi F, Mariotti L, Bi X (2012) RegT-Band: a tropical band version of RegCM4. Clim Res 52:115–133
Da Rocha RP, Morales CA, Cuandra SP, Ambrizzi T (2009) precipitation diurnal cycle and summer climatology assessment over South America: an evaluation of Regional Climate Model version 3 simulations. J Geophys Res 114:D10108, doi:10.1029/2008JD010212
Dickinson RE, Errico RM, Giorgi F, Bates GT (1989) A regional climate model for the western United States. Clim Change 15:383–422
Dickinson RE, Henderson-Sellers A, Kennedy P (1993) Biosphere–atmosphere transfer scheme (BATS) version 1e as coupled to the NCAR community climate model. Tech Rep, National Center for Atmospheric Research Tech Note NCAR.TN-387+STR, NCAR, Boulder, CO
Diro GT, Rausher SA, Giorgi F, Tompkins AM (2012) Sensitivity of seasonal climate and diurnal precipitation over Central America to land and sea surface schemes in RegCM4. Clim Res 52:31–48
Emanuel KA (1991) A scheme for representing cumulus convection in large-scale models. J Atmos Sci 48:2313–2335
Emanuel KA, Zivkovic-Rothman M (1999) Development and evaluation of a convection scheme for use in climate models. J Atmos Sci 56:1766–1782
Fairall CW, Bradley EF, Godfrey JS, Wick GA, Edson JB, Young GS (1996) Cool-skin and warm-layer effects on sea surface temperature. J Geophys Res 101:1295–1308
Gao XJ, Zhao ZC, Ding YH, Huang RH, Giorgi F (2001) Climate change due to greenhouse effects in China as simulated by a regional climate model. Adv Atmos Sci 18:1224–1230
Gao XJ, Xu Y, Zhao ZC, Pal JS, Giorgi F (2006) On the role of resolution and topography in the simulation of East Asia precipitation. Theor Appl Climatol 86:173–185
Gao XJ, Shi Y, Song RY, Giorgi F, Wang YG, Zhang DF (2008) Reduction of future monsoon precipitation over China: comparison between a high resolution RCM simulation and the driving GCM. Meteorol Atmos Phys 100:73–86
Giorgi F (1990) Simulation of regional climate using a limited area model nested in a general circulation model. J Clim 3:941–963
Giorgi F (2006) Regional climate modeling: status and perspectives. J Phys IV 139:101–118
Giorgi F, Mearns LO (1999) Introduction to special section: regional climate modeling revisited. J Geophys Res 104:6335–6352
Giorgi F, Marinucci MR, Bates G (1993a) Development of a second generation regional climate model (RegCM2). I. Boundary layer and radiative transfer processes. Mon Weather Rev 121:2794–2813
Giorgi F, Marinucci MR, Bates G, DeCanio G (1993b) Development of a second generation regional climate model (RegCM2). II. Convective processes and assimilation of lateral boundary conditions. Mon Weather Rev 121:2814–2832
Giorgi F, Huang Y, Nishizawa K, Fu C (1999) A seasonal cycle simulation over eastern Asia and its sensitivity to radiative transfer and surface processes. J Geophys Res 104:6403–6423
Giorgi F, Bi X, Qian Y (2002) Direct radiative forcing and regional climatic effects of anthropogenic aerosols over East Asia: a regional coupled climate/chemistry-aerosol model study. J Geophys Res 107:4439, doi:10.1029/2001JD001066
Giorgi F, Francisco R, Pal JS (2003) Effects of a sub-grid scale topography and landuse scheme on surface climate and hydrology. I. Effects of temperature and water vapor disaggregation. J Hydrometeorol 4:317–333
Giorgi F, Bi X, Pal JS (2004) Mean, interannual variability and trends in a regional climate change experiment over Europe. I. Present-day climate (1961–1990). Clim Dyn 22:733–756
Giorgi F, Pal JS, Bi X, Sloan L, Elguindi N, Solmon F (2006) Introduction to the TAC special issue: the RegCNET network. Theor Appl Climatol 86:1–4
Giorgi F, Jones C, Asrar G (2009) Addressing climate information needs at the regional level: the CORDEX framework. WMO Bull 58:175–183
Grell GA (1993) Prognostic evaluation of assumptions used by cumulus parameterizations. Mon Weather Rev 121:764–787
Grell G, Dudhia J, Stauffer DR (1994) A description of the fifth generation Penn State/NCAR Mesoscale Model (MM5). National Center for Atmospheric Research Tech Note NCAR/TN-398 + STR, NCAR, Boulder, CO
Grenier H, Bretherton CS (2001) A moist PBL parameterization for large scale models and its application to subtropical cloud-topped marine boundary layers. Mon Weather Rev 129:357–377
Guenther A, Karl T, Harley P, Wiedinmyer C, Palmer PI, Geron C (2006) Estimates of global terrestrial isoprene emissions using MEGAN (Model of Emissions of Gases and Aerosols from Nature). Atmos Chem Phys 6:3181–3210
Holtslag A, de Bruijn E, Pan HL (1990) A high resolution air mass transformation model for short-range weather forecasting. Mon Weather Rev 118:1561–1575
Hostetler SW, Bates GT, Giorgi F (1993) Interactive nesting of a lake thermal model within a regional climate model for climate change studies. J Geophys Res 98:5045–5057
Huffman GJ, Adler RF, Arkin P, Chang A and others (1997) The Global Precipitation Climatology Project (GPCP) combined precipitation dataset. Bull Am Meteorol Soc 78:5–20
Huffman GJ, Bolvin DT, Nelkin EJ, Wolff DB and others (2007) The TRMM multisatellite precipitation analysis (TMPA): quasi-global, multiyear, combined-sensor precipitation estimates at fine scales. J Hydrometeorol 8:38–55
Im ES, Coppola E, Giorgi F, Bi X (2010) Validation of a high resolution regional climate model for the Alpine region and effects of a sub-grid scale topography and land use parameterization. J Clim 23:1854–1873
Jacob D, Bärring L, Christensen OB, Christensen JH and others (2007) An intercomparison of regional climate models for Europe: design of the experiments and model performance. Clim Change 81:31–52
Kiehl J, Hack J, Bonan G, Boville B, Breigleb B, Williamson D, Rasch P (1996) Description of the NCAR Community Climate Model (CCM3). National Center for Atmo-

spheric Research Tech Note NCAR/TN-420+STR, NCAR, Boulder, CO
Kok JF (2011) A scaling theory for the size distribution of emitted dust aerosols suggests climate models underestimate the size of the global dust cycle. Proc Natl Acad Sci USA 108:1016–1021
Konare A, Zakey AS, Solmon F, Giorgi F, Rauscher S, Ibrah S, Bi X (2008) A regional climate modeling study of the effect of desert dust on the west African monsoon. J Geophys Res 113:D12206, doi:10.1029/2007JD009322
Koster RD, Dirmeyer PA, Guo Z, Bonan G and others (2004) regions of strong coupling between soil moisture and precipitation. Science 305:1138–1140
Kueppers LM, Snyder MA, Sloan LC, Cayan D and others (2008) Seasonal temperature response to land-use change in the western United States. Glob Planet Change 60: 250–264
Laurent B, Marticorena B, Bergametti G, Leon JF, Mahowald NM (2008) Modeling mineral dust emissions from the Sahara desert using new surface properties and soil database. J Geophys Res 113:D14218, doi:10.1029/2007 JD009484
Malavelle F, Pont V, Mallet M, Solmon F, Johnson B, Leon JF, Liousse C (2011) Simulation of aerosol radiative effects over West Africa during DABEX and AMMA SOP-0. J Geophys Res 116:D08205, doi:10.1029/2010JD014829
Marshall J, Adcroft A, Hill C, Perelman L, Heisey C (1997a) A finite-volume, incompressible Navier Stokes model for studies of the ocean on parallel computers. J Geophys Res 102:5753–5766
Marshall J, Hill C, Perelman L, Adcroft A (1997b) Hydrostatic, quasi-hydrostatic, and nonhydrostatic ocean modeling. J Geophys Res 102:5733–5752
New MG, Hulme M, Jones PD (2000) Representing twentieth century space time climate fields. Part II: Development of a 1901–1996 mean monthly terrestrial climatology. J Clim 13:2217–2238
Oleson KW, Dai Y, Bonan G, Bosilovich M and others (2004) Technical description of the Community Land Model. National Center for Atmospheric Research Tech Note NCAR/TN-461+STR, NCAR, Boulder, CO
Oleson KW, Niu Gy, Yang ZL, Lawrence DM and others (2008) Improvements to the Community Land Model and their impact on the hydrologic cycle. J Geophys Res 113: G01021, doi:10.1029/2007JD000563
Pal JS, Giorgi F, Bi X, Elguindi N and others (2007) Regional climate modeling for the developing world: the ICTP RegCM3 and RegCNET. Bull Am Meteorol Soc 88:1395–1409
Pal JS, Small E, Eltahir E (2000) Simulation of regional-scale water and energy budgets: representation of subgrid cloud and precipitation processes within RegCM. J Geophys Res 105:29579–29594
Qian JH (2008) Why precipitation is mostly concentrated over islands in the maritime continent. J Atmos Sci 65:1428–1441
Qian JH, Robertson AW, Moron V (2010) Interactions among ENSO, the monsoons, and diurnal cycle in rainfall variability over Java, Indonesia. J Atmos Sci 67:3509–3524
Ratnam JV, Giorgi F, Kaginalkar A, Cozzini S (2009) Simulation of the Indian monsoon using the RegCM3-ROMS regional coupled model. Clim Dyn 33:119–139
Rauscher SA, Coppola E, Piani C, Giorgi F (2010) Resolution effect of regional climate model simulation of precipitation over Europe. I. Seasonal. Clim Dyn 35:685–711
Santese M, Perrone MR, Zakey AS, De Tomasi F, Giorgi F (2010) Modeling of Saharan dust outbreaks over the Mediterranean by RegCM3: case studies. Atmos Chem Phys 10:133–156
Shchepetkin AF, McWilliams JC (2005) The regional ocean modeling system (ROMS): a split-explicit, free-surface, topography-following-coordinate oceanic model. Ocean Model 9:347–404
Small EE, Sloan LC, Hostetler SW, Giorgi F (1999) Simulating the water balance of the Aral Sea with a coupled regional climate–lake model. J Geophys Res 104:6583–6602
Solmon F, Mallet M, Elguindi N, Giorgi F, Zakey A, Konaré A (2008) Dust aerosol impact on regional precipitation over western Africa, mechanisms and sensitivity to absorption properties. Geophys Res Lett 35:L24705, doi:10.1029/2008GL035900
Solmon F, Giorgi F, Liousse C (2006) Aerosol modeling for regional climate studies: application to anthropogenic particles and evaluation over a European/African domain. Tellus Ser B Chem Phys Meterol 58:51–72
Steiner AL, Pal JS, Rauscher SA, Bell JL and others (2009) Land surface coupling in regional climate simulations of the West Africa monsoon. Clim Dyn 33:869–892
Sylla MB, Coppola E, Mariotti L, Giorgi F, Ruti PM, Dell'Aquila A, Bi X (2010) Multiyear simulation of the African climate using a regional climate model (RegCM3) with the high resolution ERA-interim reanalysis. Clim Dyn 35:231–247
Tawfik AB, Steiner AL (2011) The role of soil ice in land–atmosphere coupling over the United States: a soil moisture precipitation winter feedback mechanism. J Geophys Res 116:D02113, doi:10.1029/2010JD014333
Tiedtke M (1989) A comprehensive mass-flux scheme for cumulus parameterization in large-scale models. Mon Weather Rev 117:1779–1800
Torma C, Coppola E, Giorgi F, Bartoly J, Pongracz R (2011) Validation of a high resolution version of the regional climate model RegCM3 over the Carpathian basin. J Hydrometeorol 12:84–100
Tummon F, Solmon F, Liousse C, Tadross M (2010) Simulation of the direct and semidirect aerosol effects on the southern Africa regional climate during the biomass burning season. J Geophys Res 115:D19206, doi:10.1029/2009JD013738
Uppala S, Dee D, Kobayashi S, Berrisford P, Simmons A (2008) Towards a climate data assimilation system: status update of ERA-Interim. ECMWF Newsl 115:12–18
Zakey AS, Solmon F, Giorgi F (2006) Implementation and testing of a desert dust module in a regional climate model. Atmos Chem Phys 6:4687–4704
Zakey AS, Giorgi F, Bi X (2008) Modeling of sea salt in a regional climate model: fluxes and radiative forcing. J Geophys Res 113:D14221, doi:10.1029/2007JD009209
Zaveri R, Peters LK (1999) A new lumped structure photochemical mechanism for large-scale applications. J Geophys Res 104:30387–30415
Zeng X, Beljaars A (2005) A prognostic scheme of sea surface skin temperature for modeling and data assimilation. Geophys Res Lett 32:L14605, doi:10.1029/2005 GL023030
Zeng X, Zhao M, Dickinson RE (1998) Intercomparison of bulk aerodynamic algorithms for the computation of sea surface fluxes using TOGA COARE and TAO data. J Clim 11:2628–2644
Zhang L, Brook JR, Vet R (2003) A revised parameterization for gaseous dry deposition in air-quality models. Atmos Chem Phys 3:2067–2082
Zhang D, Zakey AS, Gao X, Giorgi F, Solmon F (2009) Simulation of dust aerosol and its regional feedbacks over East Asia using a regional climate model. Atmos Chem Phys 9:1095–1110

Submitted: March 29, 2011; Accepted: May 27, 2011

Proofs received from author(s): January 9, 2012